

# Modelling spatiotemporal olfactory data in two steps: from binary to Hodgkin–Huxley neurones

Brigitte Quenet<sup>a,\*</sup>, Rémi Dubois<sup>a</sup>, Sevan Sirapian<sup>a</sup>, Gérard Dreyfus<sup>a</sup>,  
David Horn<sup>b</sup>

<sup>a</sup> *Laboratoire d'Electronique, Ecole Supérieure de Physique et de Chimie Industrielles de la Ville de Paris, 10 rue Vauquelin, 75005 Paris, France*

<sup>b</sup> *School of Physics and Astronomy, Tel Aviv University, Tel Aviv 69978, Israel*

Accepted 22 August 2002

---

## Abstract

Network models of synchronously updated McCulloch–Pitts neurones exhibit complex spatiotemporal patterns that are similar to activities of biological neurones in phase with a periodic local field potential, such as those observed experimentally by Wehr and Laurent (1996, *Nature* 384, 162–166) in the locust olfactory pathway. Modelling biological neural nets with networks of simple formal units makes the dynamics of the model analytically tractable. It is thus possible to determine the constraints that must be satisfied by its connection matrix in order to make its neurones exhibit a given sequence of activity (see, for instance, Quenet et al., 2001, *Neurocomputing* 38–40, 831–836). In the present paper, we address the following question: how can one construct a formal network of Hodgkin–Huxley (HH) type neurones that reproduces experimentally observed neuronal codes? A two-step strategy is suggested in the present paper: first, a simple network of binary units is designed, whose activity reproduces the binary experimental codes; second, this model is used as a guide to design a network of more realistic formal HH neurones. We show that such a strategy is indeed fruitful: it allowed us to design a model that reproduces the Wehr–Laurent olfactory codes, and to investigate the robustness of these codes to synaptic noise.

© 2002 Elsevier Science Ireland Ltd. All rights reserved.

*Keywords:* Neural coding; Olfactory system; Spatiotemporal patterns; Hodgkin–Huxley model; Formal neural network; Hopfield–Little dynamics

---

## 1. Introduction

Many different coding mechanisms are usually discussed in the literature, including spiking rates, time coincidence, time ranks, spatial patterns, and

spatiotemporal patterns. In the present study, we focus on coding by spatiotemporal patterns, which seems particularly relevant to the olfactory system. Modelling of coding mechanisms involves models in a wide complexity range, from simple analytically tractable networks of binary units, to very complex networks with higher biological plausibility. It is the purpose of the present methodolo-

---

\* Corresponding author

E-mail address: [brigitte.quenet@espci.fr](mailto:brigitte.quenet@espci.fr) (B. Quenet).

gical paper to endeavour bridging the gap between these two extremes. As an illustration, we show how to reproduce exactly binary-type sequences, observed in the olfactory system, with a model network of biologically plausible neurones, when a clock (internal or external) synchronises their firing activities; the analysis of the synchronisation mechanism, and of the code readout mechanism, are beyond the scope of the paper.

We focus on a network of neurones that may be fully connected if necessary (no prior restriction on the connectivity is considered). Each neurone receives an input from a sensory stage (not modelled here); this input may be either excitatory or inhibitory. In the simplest model, the neurones are binary units. The design of this model requires addressing the following two problems:

- The direct problem, i.e. the mapping from the (sensory) input space to the (internal representation) output space. In other words, the direct problem addresses the question of the dynamical behaviour of the network defined by a given connection matrix in response to a given input. When the input is stable in time, this behaviour takes on the form of a cycle of binary activities. The elements of the cycle can be computed analytically in the case of deterministic dynamics, and the occurrence probabilities of these activities can also be computed analytically in the case of stochastic dynamics. The analytical treatment thus given provides much more insight than mere numerical computations.
- The inverse problem, i.e. the design of the network given (experimentally observed) binary codes. In other words, the inverse problem addresses the question of finding the family of connection matrices and of inputs that can elicit a given sequence of binary activities.

Our approach to the design of the model with higher biological plausibility consists in keeping the same connection matrix, i.e. the same neural architecture, and the same input vector, and investigating whether the complex units can reproduce exactly the codes generated by the simple model.

Recently, we constructed such an analytically tractable model of the antennal lobe neurones (Quenet et al., 2001), whose parameters were adjusted in order to make its units fire according to experimental data recorded on the locust antennal lobe by Wehr and Laurent (1996). Wehr and Laurent observed that different odours are encoded by specific time series, which are defined in temporal windows provided by an oscillatory local field potential (LFP). We showed that the type of behaviour observed experimentally could be reproduced by a recurrent (fully connected) neuronal model as described above, consisting of binary McCulloch–Pitts neurones and updated synchronously.

In the present paper, we suggest a method for determining the parameters of the network (connection matrix and input vector) in order to reproduce the exact codes recorded experimentally, and we show how such a model can be used as a guide to the construction of a more complex network with Hodgkin–Huxley type units.

## 2. Network of binary units

In our model, binary neurone  $i$ , ( $i \in [1, \dots, N]$ ) may either fire, ( $g_i = 1$ ), or be quiescent ( $g_i = 0$ ) in each time bin. In the experimental illustration discussed below, each time bin is a period of the LFP; the  $N$  neurones represent both projection and interneurones in the case of the locust temporal lobe.

The model may have full connectivity; it has the following Hopfield–Little dynamics (Hopfield, 1982; Peretto, 1992):

$$g_i(t+1) = H\left(\sum_j W_{ij}g_j(t) + R_i - \theta_i\right) \quad (1)$$

where  $W_{ij}$  is the general term of the synaptic connection matrix; the external input  $R_i$ , provided by the sensory stage, is assumed to be constant for the duration of the experiment;  $\theta_i$  is the threshold of neurone  $i$ ;  $H$  is the Heaviside step function.

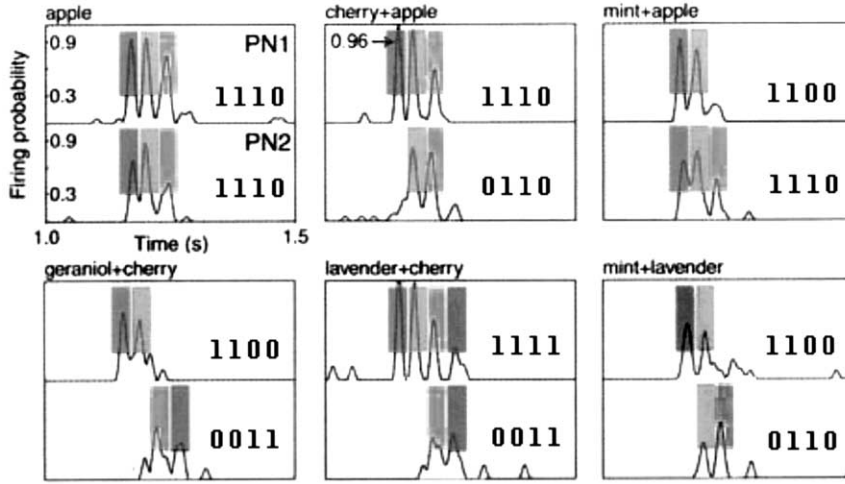


Fig. 1. Six different spatiotemporal patterns of two Projection Neurons (PN1 and PN2) firing probabilities in the locust antennal lobe, in response to six odorant inputs (from Wehr and Laurent, 1996). The firing probabilities evolve in phase with an oscillatory LFP, which defines time bins of synchronous neuronal activity. When the firing probability of a neuron is higher than 0.3 in a time bin, the authors suggest coding the activity of this neuron as 1 for the corresponding time bin and as 0 otherwise: these binary codes are indicated for each neuron and each pattern.

### 3. Direct and inverse problems

The direct problem (input–output mapping) has been analysed in detail elsewhere (Quenet et al., 1999; Quenet and Horn, 2002).

In the present study, we focus on the inverse problem: for a given set of spatiotemporal activity patterns of  $n$  neurones observed for  $T$  time steps, find a synaptic matrix  $W$  and a corresponding set of inputs  $\vec{R}_s$  that lead to the observed patterns. If the inverse problem cannot be solved with the set of observed neurones, the system can be expanded by allowing for additional, ‘hidden’, neurones whose activity has not been observed in the course of the neurophysiological experiments. In that case we look for a parsimonious model that allows for the existence of a solution to the inverse problem (a similar approach, in a different context, has been developed in Plouraboué et al., 1992).

Given a sequence, from  $t = 1$  to  $T$ , the condition for the network to generate this sequence is:

$$\sum_{j=0}^N W_{ij}g_j(t) > 0 \quad \text{if} \quad g_i(t+1) = 1, \quad (2)$$

$$i \in \{0, 1, \dots, N\}$$

$$\sum_{j=0}^N W_{ij}g_j(t) < 0 \quad \text{if} \quad g_i(t+1) = 0, \quad (3)$$

$$i \in \{0, 1, \dots, N\}$$

where  $N$  is the total number of neurones (observed and hidden),

$$W_{i0} = R_i - \theta_i \quad (4)$$

and  $g_0 = 1, \forall t$ . This set of  $T$  inequalities for each neurone can be expressed as in the conventional linear separability condition of perceptrons:

$$\vec{W}_i \cdot \vec{x}_{i,t} > 0 \quad (5)$$

where  $\vec{W}_i$  is the vector of the inputs to neurone  $i$  (the  $i$ th row of matrix  $W$ ), and  $\vec{x}_{i,t}$  is a ternary vector whose general term,  $x_{i,t,j} \in \{-1, 0, 1\}$  is defined as:

$$x_{i,t,j} = (2g_i(t+1) - 1) \cdot g_j(t) \quad (6)$$

Thus the  $(N, N+1)$  matrix  $W$  is subject to  $NT$  constraints. The initial assumption is that  $N = n$ , i.e. we are only dealing with the observed neurones, whose spatiotemporal activity is known. We consider that all neurones, except  $g_0$ , are quiescent initially:  $g_i(t=0) = 0, i = 1, \dots, N$ . We solve the

Table 1

Possible binary activities of three hidden neurones allowing a solution, with  $N = 5$ , of the Wehr–Laurent problem

Neurone	Sequence											
	$t =$	1 2 3 4	$t =$	1 2 3 4	$t =$	1 2 3 4	$t =$	1 2 3 4	$t =$	1 2 3 4	$t =$	1 2 3 4
$g_1 = \text{PN1}$		1 1 1 0		1 1 1 0		1 1 0 0		1 1 0 0		1 1 1 1		1 1 0 0
$g_2 = \text{PN2}$		1 1 1 0		0 1 1 0		1 1 1 0		0 0 1 1		0 0 1 1		0 1 1 0
$g_3 = \text{H1}$		0 0 0 0		0 0 0 0		1 1 1 1		0 1 1 1		1 0 1 1		0 1 1 0
$g_4 = \text{H2}$		0 0 1 1		0 0 1 1		0 1 1 1		0 0 0 1		1 0 0 1		0 0 1 1
$g_5 = \text{H3}$		0 1 1 0		0 1 1 0		0 0 0 0		0 0 0 0		0 0 0 1		0 0 1 0

PN1 and PN2 are the experimentally recorded neurones, H1, H2 and H3 are hidden units.

problem by considering each row of matrix  $W$  individually. For each row, the set of constraints represented by the  $(T, N+1)$  matrix  $x_i$  can be viewed as  $T$  data points in an  $N+1$  dimensional space for which the Perceptron inequality (Eq. (5)) must hold. Thus, finding a solution of the inverse problem is equivalent to finding the appropriate weights of the corresponding Perceptron.

#### 4. The Wehr–Laurent inverse problem

In Fig. 3 of their paper, Wehr and Laurent (1996) display an example of the response of two specific neurones to nine mixtures of odours. Significant results were obtained during the first four reverberations of the (LFP). They can be presented as six different binary patterns (active/inactive), as shown in Fig. 1, obtained by thresholding the firing probabilities, with a threshold of 0.3. Therefore, each pair of temporal patterns can be viewed as a spatiotemporal code for the corresponding odour.

The inverse problem defined by the data of Fig. 1 cannot be solved without introducing hidden neurones, since the deterministic dynamics of Eq. (1) cannot lead to repeating the three [1 1] states of pattern number 1 unless the system is in a fixed point (which is obviously not the case in this sequence). Therefore, this inverse problem requires at least two hidden neurones. For any given sequence, which leads to the set of constraints  $\bar{x}_{i,t}$ , the existence of a solution to the set of inequalities (5) is investigated by using the Ho–

Kashyap algorithm (Ho and Kashyap, 1965). We used the following procedure: starting with all neurones in a quiescent state (except for the bias  $g_0$ ), the first states of the hidden neurones were chosen arbitrarily. The resulting constraints were determined, and the next states were chosen appropriately, using at each step the Ho–Kashyap algorithm to find the allowed activities of the hidden neurones, thus taking into account the constraints introduced by the previously chosen states. Each choice of states leads to new constraints  $\bar{x}_{i,t}$ , some of which may be repeated, or be combinations of existing ones. At each step, the states that introduced the smallest number of *new* constraints were chosen. Through this greedy stepwise procedure, an appropriate sequence of activities was found.

Table 1 presents a result derived in the manner outlined above, with three hidden neurones.

Once the full set of sequences for all neurones (hidden and observed) is known, the possible solution of the synaptic matrix compatible with this set can be derived, using a Perceptron. For instance, a possible solution for matrix  $W$ , and six input vectors that lead to the dynamics of Table 1, are given in the caption of Fig. 3.

In this section, we showed how to design a fully connected network of binary neurones that reproduces experimentally observed codes, namely the codes observed by Wehr and Laurent in the olfactory system. In the next section we show how to use this network as a guide to designing a more biologically plausible model based on Hodgkin–Huxley (HH) type neurones.

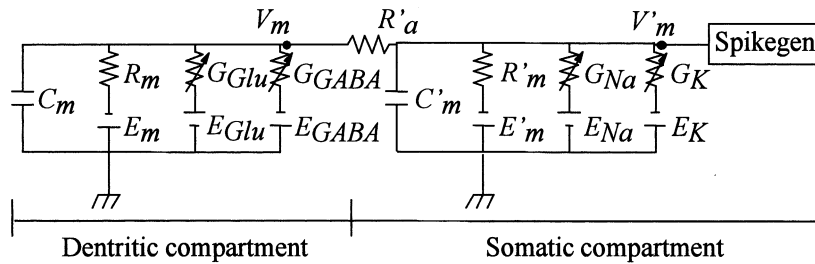


Fig. 2. Genesis two-compartment representation of a Hodgkin–Huxley neurone, with spikegen as an axonal type module.

## 5. Network of Hodgkin–Huxley neurones

The network of HH neurones was constructed with Genesis (Bower and Beeman, 1998), keeping the same synaptic matrix and the same inputs as the above model. This approach provides a powerful guide for the design of the HH network: otherwise, the problem of finding all the parameters involved in the network described below would have been essentially intractable. The neuronal units were as simple as possible, with a somatic compartment and a single dendritic one; an axonal element was added to trigger the synaptic activities according to spike emission. The neurones were synchronised by an external clock, implemented as a periodic input.

### 5.1. Neurone and synapses

The two compartments of each HH neurone are shown in Fig. 2; the list of parameters and equations used for the simulation of this neurones are given in Appendix A, and the values of the parameters are displayed in Table 2. The somatic compartment comprises sodium and potassium ionic channels. The dendritic compartment comprises inhibitory (GABA: GABAergic) and excitatory (Glu: Glutamatergic) synaptic channels, corresponding respectively to the negative and the positive values of the connection matrix.<sup>1</sup> The membrane potentials at dendritic and somatic levels of the formal neurone are solutions of

coupled differential equations (Eqs. (A-4) and (A-5) in Appendix A). The spike emission corresponds to the detection of the membrane depolarisation at the somatic level.

### 5.2. Network

The connections between neurones occur through synapses (whose response is given by Eq. (A-3)). Each synaptic connection  $S$  has two parameters: its weight  $W_S$ , and its delay  $D_S$  between a spike emission and a pre-synaptic engaging. In order to take advantage of the results of the simple model, three constraints were taken into account:

- two action potentials emitted simultaneously should elicit simultaneous responses in both excitatory and inhibitory synapses, around the next time step defined by the external clock;
- when the same number of excitatory and inhibitory synapses<sup>2</sup> are activated, no action potential should be emitted by the post-synaptic neurone; conversely, if the number of activated excitatory synapses exceeds the number of inhibitory synapses by one or more, an action potential should be emitted;<sup>3</sup>
- the model is of first order: its present activity depends only on its activity at the previous time step, i.e. its memory does not exceed one time step.

<sup>1</sup> At the antennal lobe level, both excitatory and inhibitory synapses are found: the first are essentially related to the afferent receptor cell axons and the second to the interneurons.

<sup>2</sup> Because conductances are additive,  $M$  synapses of weight 1 are equivalent to one synapse of weight  $M$ .

<sup>3</sup> Inputs and thresholds are considered as acting through synapses too.

Table 2  
Numerical values of parameters in Genesis HH model

$G_{\text{Na}}^{\text{max}}$	$G_{\text{K}}^{\text{max}}$	$G_{\text{Glu}}^{\text{max}}$	$G_{\text{GABA}}^{\text{max}}$	$X_{\text{power}}^{\text{NA}}$	$Y_{\text{power}}^{\text{NA}}$	$X_{\text{power}}^{\text{Glu}}$	$Y_{\text{power}}^{\text{Glu}}$	$\tau_{\text{Glu}}$	$\tau_{\text{GABA}}$
3.4 $\mu\text{S}$	1 $\mu\text{S}$	$5 \times 10^{-10}$ S	$5 \times 10^{-10}$ S	3	1	2	1	2 ms	20 ms
$E_{\text{m}}$	$E_{\text{m}}'$	$C_{\text{m}}$	$C_{\text{m}}'$	$R_{\text{m}}$	$R_{\text{m}}'$	$E_{\text{Na}}$	$E_{\text{K}}$	$E_{\text{Glu}}$	$E_{\text{GABA}}$
-70 mV	-59 mV	6.3 pF	28.2 pF	530.5 M $\Omega$	117.9 M $\Omega$	45 mV	-70 mV	45 mV	-90 mV
$R_{\text{a}}'$	$G_{\text{Glu}}^0$	$G_{\text{GABA}}^0$	$D_{\text{Glu}}$	$D_{\text{GABA}}$	$f_{\text{c}}$	$V_{\text{th}}$	$t_{\text{abs}}$	$\alpha_{\text{Na}}, \beta_{\text{Na}}$	$\alpha_{\text{K}}, \beta_{\text{K}}$
12.7 k $\Omega$	10 nS	24 nS	0.2 ms	0.18 ms	5 Hz	0.5 mV	0.05 s	Na-mit-usb	K-mit-usb

'Na-mit-usb' and 'K-mit-usb' are names of modules available in Genesis.

In order to satisfy the first constraint, slightly different values must be assigned to the synaptic delays of the excitatory ( $D_{\text{Glu}}$ ) and inhibitory synapses ( $D_{\text{GABA}}$ ): this guarantees that the conductance responses to action potentials emitted simultaneously by pre-synaptic neurones reach their maximum simultaneously around the next time step of the external clock.

The second constraint requires to define appropriately a maximal synaptic conductance for excitatory ( $G_{\text{Glu}}^0$ ) and inhibitory synapses ( $G_{\text{GABA}}^0$ ), which will serve as unit values for each type of synapse, in order to make sure that: (i) an inhibitory synapse of weight  $M$  will compensate the effect of an excitatory synapse of same weight; and that (ii) a single extra unit excitation will drive a spiking behaviour of the post-synaptic neurone; this should hold in a large range of values of  $M$ , typically from 1 to 200. In other words, a synapse of weight  $M$  in the network of simple binary units corresponds to a synapse of weight  $MG_{\text{Glu}}^0$  in the network of HH units if  $M$  is positive, and  $MG_{\text{GABA}}^0$  if  $M$  negative. Therefore, when the values  $G_{\text{Glu}}^0$  and  $G_{\text{GABA}}^0$  are appropriate,  $MG_{\text{Glu}}^0$  and  $MG_{\text{GABA}}^0$  applied on the same neurone do not elicit any action potential, while  $(M+1)G_{\text{Glu}}^0$  and  $MG_{\text{GABA}}^0$  elicit an action potential. Hence, in order to relate the analytically tractable network to the more biologically plausible one, each positive value of synaptic connections,  $W_{ij}$ , is represented by a maximal synaptic conductance  $W_{ij}G_{\text{Glu}}^0$ , and each negative synaptic connection is represented by a maximal synaptic conductance  $W_{ij}G_{\text{GABA}}^0$ . Finally, in order to make sure that the network 'memory' does not exceed one time step, the external clock frequency  $f_{\text{c}}$  should be low enough

that, before any new pre-synaptic spike, all synaptic conductances are reset to zero.

### 5.3. Inputs and threshold

Two synchronous generators emit regular spikes at frequency  $f_{\text{c}}$ ; one generator sends spikes to the excitatory synapses of the neurones, while the other sends spikes to their inhibitory synapses, in order to take into account the positive and negative values of the  $\bar{R}$ s (in caption of Fig. 3). As mentioned for the synaptic connection values, each input value (with 0.5 subtracted, the value of the threshold  $\theta_i$  of the formal model) is multiplied by the corresponding maximal synaptic conductance, i.e.  $G_{\text{Glu}}^0$  for positive values and  $G_{\text{GABA}}^0$  for negative ones; hence an input  $R_i$  on neurone  $i$  in the network of binary neurones corresponds to a maximal synaptic conductance  $R_iG_{\text{Glu}}^0$  if  $R_i$  is positive or to  $R_iG_{\text{GABA}}^0$  if  $R_i$  is negative.

## 6. Simulation results

Genesis simulations were performed on the model described above, by applying the exponential Euler integration method with an integration time step of 0.01 ms.<sup>4</sup> All  $N = 5$  formal neurones were initially inactive; an input was applied to the synapses at time  $t = 0.2$  sec, which corresponds to discrete time  $t = 1$  in the binary neural model. Fig. 3 shows the six simulated recordings of the

<sup>4</sup> The value of the integration time step is not critical and can be varied between 0.001 and 0.1 ms without any significant change in the results.

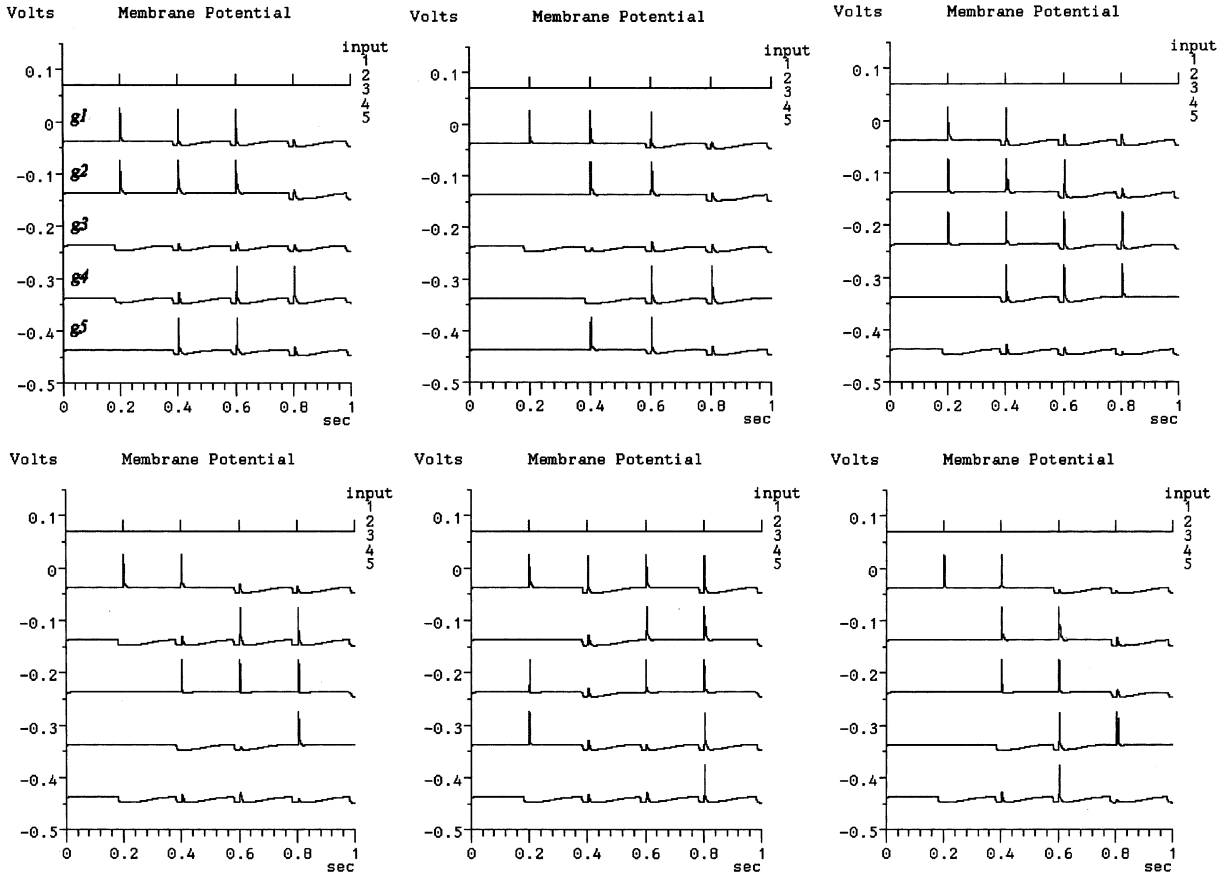


Fig. 3. Six different spatiotemporal patterns obtained with a Genesis simulation of Hodgkin–Huxley type neurones. They correspond exactly to the binary codes of Table 1, and the first two lines under the input (clock) line reproduce respectively the activities of PN1 and PN2 in the Wehr–Laurent experiment. Synapses and inputs have the following values (the threshold  $\theta_i = \theta = 0.5$  for all neurones, with the trivial state  $\vec{0}$  as initial state):

$$W = \begin{pmatrix} 0 & -2 & -5 & -3 & 0 \\ 6 & 2 & 8 & -14 & 0 \\ 1 & 1 & 0 & -2 & 1 \\ -4 & 6 & 1 & 1 & 3 \\ 4 & -1 & 2 & -4 & 0 \end{pmatrix};$$

and

$$\vec{R}^1 = \begin{pmatrix} 3 \\ 5 \\ -3 \\ -2 \\ 0 \end{pmatrix}; \quad \vec{R}^2 = \begin{pmatrix} 3 \\ 0 \\ -3 \\ 0 \\ 0 \end{pmatrix}; \quad \vec{R}^3 = \begin{pmatrix} 10 \\ 2 \\ 2 \\ 0 \\ -5 \end{pmatrix}; \quad \vec{R}^4 = \begin{pmatrix} 4 \\ -7 \\ 0 \\ 0 \\ -6 \end{pmatrix}; \quad \vec{R}^5 = \begin{pmatrix} 9 \\ 0 \\ 1 \\ 2 \\ -4 \end{pmatrix}; \quad \vec{R}^6 = \begin{pmatrix} 2 \\ 0 \\ 0 \\ 0 \\ -4 \end{pmatrix}$$

membrane potential ( $V'_m$ ) of the five neurones, in response, respectively, to the six different inputs

indicated in the caption of Fig. 3. The spiking activity of the neurones occurs at precise time bins,

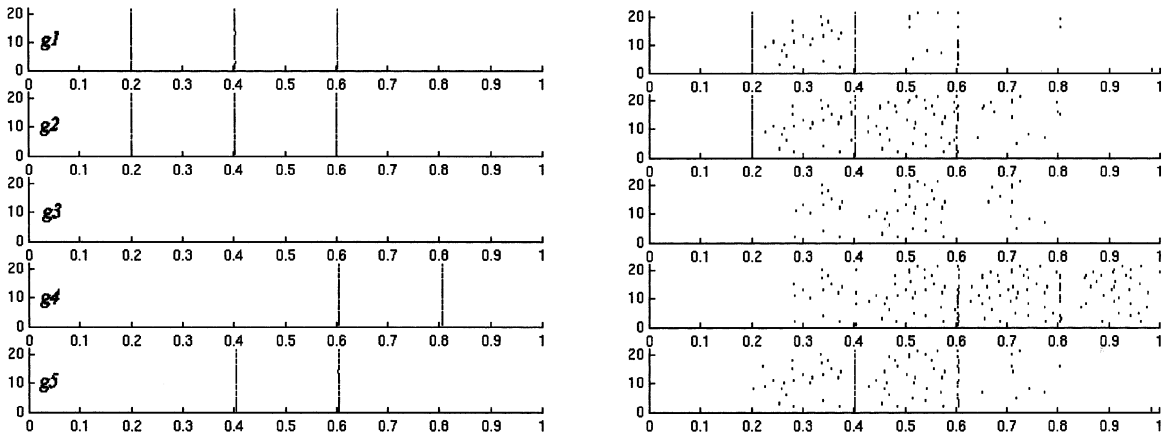


Fig. 4. Spike recordings for 21 simulations performed with input  $\vec{R}^1 = (3, 5, -3, -2, 0)$ , which leads the network to exhibit the first pattern of Table 1. Left, no noise. Right, in the presence of additional noise ( $W_n = 0.5$  and  $f_n = 10$  Hz) spurious spikes occur, but the first pattern of Table 1 are easily recognised.

corresponding to the external clock, and it reproduces exactly the binary codes of Table 1; the first two neurones fire precisely according to the firing pattern of neurones PN1 and PN2 of Wehr and Laurent's experiment. Thus, the Wehr and Laurent's experimental data was reproduced quantitatively through a simulation of Hodgkin–Huxley type neurones with appropriately tuned parameters, using the information gathered from the network of binary neurones.

### 7. Adding noise to the model

Since some parameters of the synapses had to be tuned, we investigate the robustness of the results obtained with this set of parameters to the addition of noise. In our Genesis simulations, the noise was represented by two additional input generators, one to excitatory synapses, one to inhibitory ones, whose spikes were random with a spiking rate around a given mean frequency  $f_n$ . The synaptic weights of these connections have a single module,  $W_n$ . Fig. 4 shows a set of 21 simulations performed for input  $\vec{R}^1$ ; the spikes generated during each simulation for each neurone were recorded and shown as dots. Although extra spikes are generated outside the temporal bins, the codes of pattern 1 can be clearly recognised.

### 8. Discussion and conclusion

Models of binary neurones have attracted a lot of attention because they can be analysed mathematically in a reasonably straightforward fashion, but they definitely lack biological plausibility; conversely, networks of more realistic neurones tend to be intractable, so that their analysis relies solely on computer simulations, involving numerous parameters that can vary in wide ranges of values. In the present study, we have shown that one can have the best of both worlds: the binary model allows the designer to understand in depth the principles of operation of the neural system under investigation, and it serves as a guide to the design of biologically plausible models. We have illustrated this methodology on an example of olfactory coding, and we have been able to reproduce experimental data accurately. In a more theoretical paper (Quenet and Horn, 2002) several analytical properties of a fully connected network of binary units are investigated, such as its coding capabilities, and the size and characteristics of the basins of attractions, which are related to the robustness of this type of coding against input noise. In future work, more biological plausibility will be achieved by relaxing the assumption of strict synchronisation, and by introducing the following constraints in the model: (i) the synapses of a given neurone should have a

single sign; (ii) the inputs should be positive and mimic the odorant mixtures used in the experiments. The additional coding capabilities gained through the introduction of spiking neurones will be investigated in a more detailed fashion.

## Appendix A

Each formal HH type neurone has two compartments (Fig. 2). The somatic compartment comprises sodium and potassium ionic channels, whose voltage-dependent conductance  $G_I$  (with  $I = K$  or  $I = Na$ ) obeys the following equation:

$$G_I = G_I^{\max} \cdot X^{X_{\text{power}}^I} \cdot Y^{Y_{\text{power}}^I} \quad (\text{A-1})$$

where  $G_I^{\max}$  is the maximal channel conductance,  $X$  is the ionic activation variable,  $Y$  is the ionic inactivation variable.  $X_{\text{power}}^I$  and  $Y_{\text{power}}^I$  depend on both the channel and neurone types.  $X$  and  $Y$  are functions of time  $t$  and of the membrane potential  $V_m$ ; they obey the following differential equation, where  $Z$  represents either  $X$  or  $Y$ :

$$\frac{dZ}{dt} = \alpha_Z(V'_m - V_0) \cdot [1 - Z] - \beta_Z(V'_m - V_0) \cdot Z \quad (\text{A-2})$$

where  $V_0$  is the resting potential, and both  $\alpha_Z(V'_m - V_0)$  and  $\beta_Z(V'_m - V_0)$  are tabulated and/or interpolated functions.

The dendritic compartment comprises inhibitory (GABA: GABAergic) and excitatory (Glu: Glutamatergic) synaptic channels, whose conductance response to a pre-synaptic spike at  $t = 0$  is given by:

$$G_S(t) = G_S^{\max} \cdot \frac{t}{\tau_S} \exp\left(1 - \frac{t}{\tau_S}\right) \quad (\text{A-3})$$

where  $S$  stands for either GABA or Glu.  $G_S^{\max}$  is the maximal conductance of a synapse of  $S$  type, reached when  $t = \tau_S$ , its time constant.

The membrane potentials  $V_m(t)$ ,  $V'_m(t)$ , at dendritic and somatic levels of the formal neurone respectively, are solutions of the following coupled differential equations, derived from Kirchoff's law (see Fig. 2) where the electric parameters are

$$C_m \frac{dV_m}{dt} = \frac{(E_m - V_m)}{R_m} + \sum_S [(E_S - V_m) \cdot G_S] + \frac{(V'_m - V_m)}{R_a} \quad (\text{A-4})$$

$$C'_m \frac{dV'_m}{dt} = \frac{(E'_m - V'_m)}{R'_m} + \sum_I [(E_I - V'_m) \cdot G_I] + \frac{(V_m - V'_m)}{R_a} \quad (\text{A-5})$$

The spike emission, delivered by a module 'spikegen' in Genesis, corresponds to the detection of the membrane depolarisation at the somatic level; it occurs when  $V'_m(t)$  becomes higher than  $V_{\text{th}}$ , a fixed threshold characterising the module, if the last spike was emitted before  $t_{\text{abs}}$ , an absolute refractory period.

## References

- Bower, J.M., Beeman, D., 1998. The Book of GENESIS, 2nd edition. Springer Verlag, Berlin.
- Ho, E., Kayshap, R.L., 1965. An algorithm for linear inequalities and its applications. IEEE Trans. Elect. Comp. 14, 683–688.
- Hopfield, J.J., 1982. Neural networks and physical systems with emergent collective computational abilities. Proc. Natl. Acad. Sci. USA 79, 2554–2558.
- Plouraboué, F., Atlan, H., Weisbuch, G., Nadal, J.-P., 1992. A network model of the coupling of ion channels with secondary messenger in cell signaling. Network: Comp. Neural Syst. 3 (4), 393–406.
- Peretto, P., 1992. An Introduction to the Modeling of Neural Networks. Cambridge University Press, Cambridge.
- Quenet, B., Horn, D., 2002. Dynamical neural filter: a binary model of spatiotemporal coding. Neural Comput., in press.
- Quenet, B., Dreyfus, G., Masson, C., 1999. From complex signal to adapted behavior: a theoretical approach of the honeybee olfactory brain. In: Burdet, G., Combe, P., Parodi, O. (Eds.), Series in Mathematical Biology and Medicine, vol. 7. World Scientific, London, pp. 104–126.
- Quenet, B., Horn, D., Dreyfus, G., Dubois, R., 2001. Temporal coding in an olfactory oscillatory model. Neurocomputing 38–40, 831–836.
- Wehr, M., Laurent, G., 1996. Odour encoding by temporal sequences of firing in oscillating neural assemblies. Nature 384, 162–166.